Supplementary S2

Methodology for sterlet DNA research

Ancient Samples

During excavations in the Middle and Lower Volga region between 2002 and 2016, 18 ancient sterlet bone samples were extracted from 16 archaeological sites (Fig. S1,Table S1). To establish the species identification of the samples, all sterlet bone remains were carefully examined based on their morphology. Furthermore, the samples were dated based on their archaeological context at the Biomonitoring Laboratory of the Institute of Problems in Ecology and Mineral Wealth, Tatarstan Academy of Sciences, Kazan, Russia. It is worth noting that sturgeon remains are easily identifiable due to their specific diagnostic features and dense bone structure. Additionally, the degree of preservation of fish bones and the probability of finding their remains in the layers of an archaeological site depend on the functional features of various elements of the skeleton. For instance, functionally loaded elements of the skeleton, such as *pinna pectoralis I*, are the strongest and most resistant to destruction processes ([1]. In this study, we selected the bones of the exoskeleton of the pectoral fins and their girdles—pinna pectoralis I, clavicula, and cleithrum. Sterlet size reconstruction (total length, TL) was carried out based on the regression equations that establish the relationship between the bone size and the absolute length of the fish body [2].

Contemporary Samples

Five wild samples were collected from the Kama River as part of an ecological monitoring program by the Biomonitoring Laboratory (Institute of Problems in Ecology and Mineral Wealth, Tatarstan Academy of Sciences, Kazan, Russia) (Fig. S1,Table S1. Only pectoral fin tips were used for DNA isolation.

Ancient DNA Isolation and Sequencing

All experiments in DNA isolation and sequencing were conducted in a laboratory specialized in ancient DNA at the Institute of Molecular and Cellular Biology of the Siberian Branch of the Russian Academy of Sciences (Novosibirsk, Russia), with maximum protection against contamination (use of special protective clothing, surface treatment with DNAZap nucleic acid-degrading solutions (ThermoFisher Scientific, USA), and ultraviolet irradiation of laboratory premises). All ancient bone specimens were subjected to UV irradiation (30 min on each side of the bone) to destroy the upper layer of DNA and potential DNA contamination. The bones were ground into bone powder and ancient DNA extraction was performed following the previously

described protocol using silica-based spin columns (QIAquicky, QIAGEN, Germany)[3], with some modifications according to Sanderson et al.[4]: the lysis buffer contained 0,45 M (NH4)4EDTA for reducing the decalcification time from 18–24 h to 1.5–3.0 h at a standard concentration of 300 mg of the bone powder per 5 mL of the buffer at 55°C.

PCR-mix was prepared in a specialized pre-PCR box, designed for ancient DNA experiments only.

The primers were designed using Primer-BLAST (https://www.ncbi.nlm.nih.gov/tools/primer-blast/) based on the sequence of the sterlet complete mitochondrial genome KF153104.1[5]. To analyze a 490-bp mtDNA control region fragment from the ancient samples, we amplified four overlapping short fragments from nested primers (Table S2). The amplification of each one of the four fragments was carried out in a separate PCR.

All the sterlet sequences obtained were deposited in GenBank under accession numbers OM927985-OM928002 and OM928003-OM928007 for ancient and contemporary samples, respectively (Table S3). As the region recovered by ancient samples sequencing is shorter than the haplotypes published earlier, we first checked what haplotypes were indistinguishable in this region.

Contemporary DNA Isolation and Sequencing

The isolation and sequencing of DNA from the modern samples was carried out according to the methodology given by Pobedintseva et al.[6].

Hypervariable Positions

In the previous study of sterlet mitochondrial DNA [6], six positions in the control region were listed as hypervariable. In our alignment, one position (16392) fell into the gap and, therefore, was not included in the analysis. Four positions (16330, 16339, 16465, and 16520) contained only two different nucleotides. Therefore, only one previously reported position (16163) plus one new position (16190) containing three different nucleotides should be treated as hypervariable in the current alignment. However, these two positions were included in a subsequent analysis.

Candidate Deamination Sites in Ancient Samples

Ancient DNA is well known to contain postmortem damage [7]. The most common type of damage is the deamination of cytosine, leading to C -> T and G -> A substitutions observed in the sequencing data. We classified possible deamination sites into three categories for the manual check of two peak presences in the raw Sanger data. For possible C -> T substitutions,

we followed the rules below. High-priority sites were classified based on the following: - C was present in at least one modern haplotype; - T was present in less than two ancient samples (<=2). The medium-priority sites fit the following criteria: C was present in at least one modern haplotype; T was present in more than two but in less than nine ancient samples (>2, <=9). The low-priority sites were as follows: C was present in at least one modern haplotype; T was present in more than nine ancient samples (> 9). The same rules were applied for possible G->A substitutions. The coordinates of candidate deamination sites are listed in Supplementary 2 Table 5. We manually checked the intensities in the raw Sanger reads for possible deamination events. But, even in a few high-priority candidate sites, we found only a weak background signal of possibly deaminated bases. In other words, in our data, even if it occurred in some of the original DNA fragments (before PCR), deamination did not significantly change the base content. Therefore, we included consensus sequences in the subsequent analysis.

Population Genetics' Analysis

Sequences of contemporary and ancient haplotypes were aligned to the reference full mitochondrial genome sequence KF153104.1 [5]using MAFFT v 7.450 [8]. For the ancient samples, four overlapping fragments were obtained, with 489/490 bp-consensus sequence assembled in Geneious v8.1.7 [9]. The resulting sequences (positions 16089-16578 in mtDNA with a polymorphic 1 bp deletion at position 16404) were used in a subsequent analysis. Most ancient samples had an un-sequenced gap of different lengths in the area between positions 16210 and 16262. The exact coordinates of the gaps in each sample are shown in Supplementary Table 1. Prior to the exclusion of the region containing gaps in all samples, we checked which haplotypes that had been previously obtained in Pobedintseva et al. [6] were indistinguishable with and without it. The clustering of the haplotypes was performed using CD-HIT v4.7 [10]. To form clusters, 100% identity in sequence content and length was required. Prior to the final filtration stage, the detection of hypervariable sites was performed according to previously described data [6], but, due to the low number of such sites, these were retained. In the final alignment, we removed all indistinguishable and minor haplotypes, except for the ones which had originated from the Volga basin. UGENE v34 [11] was used to perform routine manipulations with multiple alignments.

The haplotype network based on the final alignment was reconstructed using the TCS method [12]. In the final alignment, a polymorphic 1 bp deletion was left at position 16404, analyzed as an SNP in the construction of the haplotype network, and visualized using the PopArt v1.7 package [13]. The contemporary haplotypes included in this study are shown in Table S4.

The presence–absence matrix of sterlet haplogroup distribution across river basins was built using PAST software v. 4.14 [14]. The presence–absence status was recorded for all the haplotypes, and a generalized statistical result was presented for all the haplogroups included in this study.

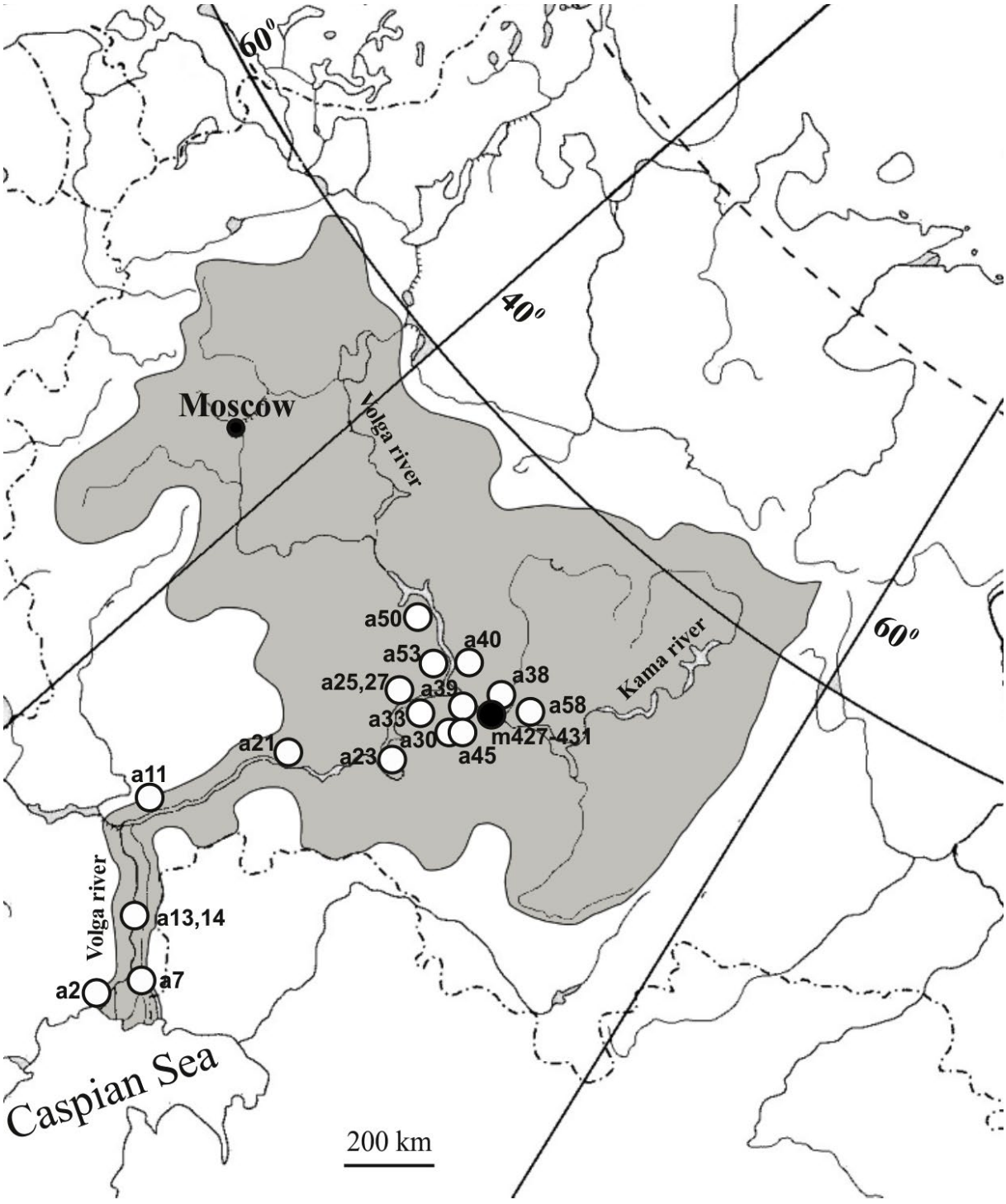

Figure S1. Map of ancient (white) and contemporary (black) sterlet sampling collection sites.

Table S1. Ancient and contemporary sterlet (*A. ruthenus*) samples.

Sequence ID	NCBI Accession numbers	Studied bone/body organ	Site name/date of excavation	Republic/ Region	Dating/ Phasing Informa-tion	Body Size (TL) *Restored Length
an34	OM927985	Clavicula	Ostolopovo settlement, 2013	The Republic of Tatarstan	end of 10th–12th cc. AD	47 cm*
an25	OM927986	Pinna pectoralis I	Tetyushskoe II hillfort, 2010	The Republic of Tatarstan	4th–8th cc. AD	48 cm*
an23	OM927987	Pinna pectoralis I	Muromsky gorodok, 2005	Samara region	10th–12th cc. AD	48 cm*
an53	OM927988	Pinna pectoralis I	Sviyazhsk, 2013	The Republic of Tatarstan	17th–18 th cc. AD	49 cm*
an21	OM927989	Pinna pectoralis I	Bagaevka settlement, 2014	Saratov region	13th–14th cc. AD	78 cm*
an13	OM927990	Pinna pectoralis I	Selitrennoye settlement, 2010	Astrakhan region	14th c. AD	79 cm*
a58	OM927991	Pinna pectoralis I	Elabuga hillfort, 2003	The Republic of Tatarstan	layers of 12th–13th cc. AD	81 cm*
an27	OM927992	Pinna pectoralis I	Tetyushskoe II hillfort, 2010	The Republic of Tatarstan	4th–8th cc. AD	63 cm*
an50	OM927993	Pinna pectoralis I	Maly Sundyr' hillfort, 2000.	Republic of Mari El	end of 13th–15th cc. AD	44 cm*
an14	OM927994	Pinna pectoralis I	Selitrennoye settlement, 2010	Astrakhan region	14th c. AD	82 cm*
an40	OM927995	Cleithrum	Kazan, territory of Kazan State University, 2002	The Republic of Tatarstan	16th–18th cc. AD	46 cm*

an33	OM927996	Pinna pectoralis I	Bulgar fortified settlement, 2016	The Republic of Tatarstan	13th–14th cc. AD	71 cm*
an38	OM927997	Pinna pectoralis I	Kirmen settlement, 2008	The Republic of Tatarstan	13th–14th cc. AD	59 cm*
an30	OM927998	Pinna pectoralis I	Bilyar fortified settlement, 2016	The Republic of Tatarstan	11th–12th cc. AD	51 cm*
an2	OM927999	Pinna pectoralis I	Samosdelka hillfort, 2008	Astrakhan region	13th–14th cc. AD	66 cm*
an11	OM928000	Pinna pectoralis I	Vodyanskoe settlement, 2010	Volgograd region	14th c. AD	77 cm*
an45	OM928001	Pinna pectoralis I	Toretskoe settlement, 2007	The Republic of Tatarstan	15th c. AD	55 cm*
an7	OM928002	Pinna pectoralis I	Moshaik hillfort, 2011	Astrakhan region	14th c.AD	68 cm*
m427	OM928003	Pectoral fin	Kama River, Rybno Slobodsky district	The Republic of Tatarstan	2020	51 cm
m428	OM928004	Pectoral fin	Kama River, Rybno Slobodsky district	The Republic of Tatarstan	2020	55 cm
m429	OM928005	Pectoral fin	Kama River, Rybno Slobodsky district	The Republic of Tatarstan	2020	65 cm
m430	OM928006	Pectoral fin	Kama River, Rybno Slobodsky district	The Republic of Tatarstan	2020	66 cm
m431	OM928007	Pectoral fin	Kama River, Rybno Slobodsky district	The Republic of Tatarstan	2020	52 cm

Table S2. The list of primers used for sterlet mtDNA sequencing.

Primer name	5'->3' primer sequence	Annealing temperature	Product length
ArF1	TGTTTCATCTACCATCAAATGATATACAC	61˚C	177 bp
ArR1	CCAGATGCCAGTAATAATTCAGTTATG	61˚C	
ArF2	TTAATGAGATGAAGGACAATACCTGTAG	61˚C	182 bp

ArR2	CCAAATGTTGGCATGGTTCTC	61˚C	
ArF3	AGGTACCATACACCCATGACCC	61˚C	144 bp
ArR3	GTCTTCGAGCAGACCGTGAAT	61˚C	
ArF4	ATGCAAAACGCTCCTTCAGAG	61˚C	161 bp
ArR4	TGGGAACAAGATTAGGTCCTGTG	61˚C	

Table S3. Accession numbers in GenBank and length of gap for ancient samples.

Sequence ID	Accession Number	Gap Length	Gap Start	Gap End
an34	OM927985	44	16210	16253
an25	OM927986	24	16229	16252
an23	OM927987	no gap	NA	NA
an53	OM927988	29	16225	16253
an21	OM927989	29	16226	16254
an13	OM927990	42	16221	16262
an58	OM927991	28	16226	16253
an27	OM927992	34	16229	16262
an50	OM927993	30	16225	16254
an14	OM927994	26	16228	16253
an40	OM927995	29	16225	16253
an33	OM927996	27	16227	16253
an38	OM927997	32	16229	16260
an30	OM927998	25	16229	16253
an2	OM927999	27	16226	16252
an11	OM928000	30	16229	16258
an45	OM928001	23	16231	16253
an7	OM928002	no gap	NA	NA

Table S4. Contemporary haplotypes included in this study.

Sequence ID	Haplotype	Haplotype Occurrence
KU984263.1	A1	a common haplotype from the Ob-Irtysh basin and very rare in Yenisei *
KU984270.1	A2	a common haplotype from the Ob-Irtysh basin *
KU984278.1	A3	a common haplotype from the Ob-Irtysh basin, rare in Yenisei *
KU984288.1	B1	a common haplotype from the Ob-Irtysh basin [6]*
KU984294.1	C1	a common haplotype from the Ob-Irtysh basin*
OM928007	C1B1	a haplotype from Kama (Volga basin) (sample m431) **
KU984301.1	D1	a common haplotype from the Ob-Irtysh basin, very rare in Yenisei *
KU984303.1	E1	a rare haplotype from Ob *
KU984304.1	E2A	a rare haplotype from Ob *
KU984305.1	E2B	a rare haplotype from Ob *
OM928005	E3A1	a haplotype from Kama (Volga basin) (sample m429) **
KU984306.1	E3A	a haplotype from Volga *
KU984307.1	E3B	a haplotype from the aquacultured samples originating from Kama *
OM928003	E3G	a haplotype from Kama (Volga basin) (sample m427) **
OM928004	F2	a haplotype from Kama (Volga basin) (sample m428) **
OM928006	F3	a haplotype from Kama (Volga basin) (sample m430) **
KU984308.1	F1	a rare haplotype from Ob *
KU984309.1	G	a very rare haplotype (from a monotypic clade) from Irtysh *
KU984310.1	H	a haplotype from the aquacultured samples originating from Kama *
KU984311.1	I1	a common haplotype from the Ob-Irtysh basin *

KU984317.1	I3	a rare haplotype from Ob *
KU984323.1	I4	a common haplotype from the Ob-Irtysh basin *
KU984328.1	J	a very rare haplotype (from a monotypic clade) from Irtysh *
KU984329.1	K	a very rare haplotype (from a monotypic clade) from Ob *
KU984330.1	L	a very rare haplotype (from a monotypic clade) from Irtysh *

* Obtained by [6].

** Obtained in this study.

Table S5. Coordinates of deamination sites in ancient samples.

	High priority		**Medium priority**		**Low priority**	
	C->T	**G->A**	**C->T**	**G->A**	**C->T**	**G->A**
Coordinates in trimmed alignment without un-sequenced gap	65 175 262 263 327 368 383	118 146 252 298 325 333 334 354	56 57 69 227 323	104 115 207 251 339 342	5 9 63 75 98 142 144 209 219 307 320 326 341 374 379 406	18 23 25 55 58 64 67 73 74 99 116 131 134 145 161 204 242 248 250 265 299 322 347 371 378 380 398 407
Coordinates in reference (KF153104.1)	16153 16263 16350 16351 16469 16510 16525	16206 16234 16340 16440 16467 16475 16476 16496	16144 16145 16157 16315 16465	16192 16203 16295 16339 16481 16484	16093 16097 16151 16163 16186 16230 16232 16297 16307 16449 16462 16468 16483 16516 16521 16548	16106 16111 16113 16143 16146 16152 16155 16161 16162 16187 16204 16219 16222 16233 16249 16292 16330 16336 16338 16353 16441 16464 16489 16513 16520 16522 16540 16549

References Supplementary S2

1. Askeyev, I.V.; Galimova, D.N.; Askeyev, O.V. Ichthyofauna of the middle Volga River basin in the Late Holocene (based on archaeological excavations). *Zool. Zhurnal* **2013**, *92*, 1014–1030. https://doi.org/10.7868/S0044513413090043.
2. Shaymuratova, D.N.; Askeyev, I.V.; Askeyev, O.V.; Monachov, S.P.; Askeyev, A.O.; Smirnov, A.A. Sterlet Acipenser ruthenus (*Acipenseriformes, Acipenseridae*) of Middle Volga and Lower Kama in IV–XVIII centuries AD: Size and age composition, growth and value in the ancient fishing. *Vopr. Rybolov.* **2017**, *18*, 401–421.
3. Yang, D.Y., Eng, B., Waye, J.S., et al. Technical Note: Improved DNA Extraction From Ancient Bones Using Silica-Based Spin Columns, Am. J. Phys. Anthropol., **1998**,*105*, 539–543. https://doi.org/10.1002/(SICI)1096-8644(199804)105:4<539::AID-AJPA10>3.0.CO;2-1
4. Sanderson, C., Radley, K., and Mayton, L.,1995. Ethylenediaminetetraacetic acid in ammonium hydroxide for reducing decalcification time, Biotech. Histochem., **1995**, *70*(*1*), 12–18. https://doi.org/10.3109/10520299509108310
5. Li, C., Cheng, L., Li, J-T., et al. 2013. Complete mitochondrial genome of sterlet (*Acipenser ruthenus*). Mitochondrial DNA, **2013**, *26*(*2*), 259–260. https://doi.org/10.3109/19401736.2013.823188
6. Pobedintseva, M.A.; Makunin, A.I.; Kichigin, I.G.; Kulemzina, A.I.; Serdyukova, N.A.; Romanenko, S.A.; Vorobieva, N.V.; Interesova, E.A.; Korentovich, M.A.; Zaytsev, V.F.; et al. Population genetic structure and phylogeography of sterlet (Acipenser ruthenus, Acipenseridae) in the Ob and Yenisei river basins. *Mitochondrial DNA Part A* **2019**, *30*(*1*) 156–164. https://doi.org/10.1080/24701394.2018.1467409
7. Dabney J, Meyer M, Pääbo S. Ancient DNA damage. Cold Spring Harb Perspect Biol., **2013**, *5*. a012567, 1-9. https://doi.org/doi:10.1101/cshperspect.a01256
8. Katoh, K., and Standley, D.M. MAFFT multiple sequence alignment software version 7: Improvements in performance and usability, Mol. Biol. Evol., **2013**, (*30*)*4*, 772–780. https://doi.org/10.1093/molbev/mst010
9. Kearse, M., Moir, R., Wilson, A., et al. Geneious Basic: An integrated and extendable desktop software platform for the organization and analysis of sequence data, Bioinform., **2012**, (*28*),*12*, 1647–1649. https://doi.org/10.1093/bioinformatics/bts199
10. Fu, L., Niu, B., Zhu, Z., et al. CD-HIT: Accelerated for clustering the next-generation sequencing data, Bioinform., **2012**, (*28*)*23*, 150–3152. https://doi.org/10.1093/bioinformatics/bts565
11. Okonechnikov, K., Golosova, O., Fursov, M., et al. Unipro UGENE: A unified bioinformatics toolkit, Bioinform., **2012**, (*28*) *8*, 1166–1167. http://dx.doi.org/10.1093/bioinformatics/bts091
12. Clement, M., Snell, Q., Walker, P., et al. TCS: estimating gene genealogies. Parallel and Distributed Processing Symp. International, 2002,3, 184–190.
13. Leigh, J.W., and Bryant, D. POPART: Full-feature software for haplotype network construction, Methods. Ecol. Evol., **2015**. (*6*)*9*, 1110–1116. https://doi.org/10.1111/2041-210X.12410
14. Hammer, O.; Harper, D.A.T.; Ryan, P.D. PAST: Paleontological Statistics Software Package for Education and Data Analysis. *Palaeontol. Electron.* **2001**, *4*, 1–9.